# Modelling Techniques for Buffeting Analysis of Long-span Bridges

**Igor KAVRAKOV**
Graduate Student
Bauhaus-University
Weimar, Germany
*igor.kavrakov@uni-weimar.de*

**Guido MORGENTHAL**
Professor
Bauhaus-University
Weimar, Germany
*guido.morgenthal@uni-weimar.de*

## Summary

Wind-induced vibrations commonly represent the leading criterion in the design of long-span bridges. By well accepted classification, the aerodynamic forces are categorized into static, self-excited and buffeting forces for which different formulations apply based on the quasi-steady and the linear unsteady air-foil theory. This paper aims to investigate different formulations of the self-excited and buffeting forces in time domain by comparing the dynamic response of a cable-stayed bridge during the critical erection condition. The models are viewed from a complexity perspective, comparing the assumptions implied such as aerodynamic damping, admittance, fluid memory, aerodynamic nonlinearity and aerodynamic coupling. These are quantified based for design wind-speeds which are typical for the construction stage.

**Keywords:** Wind-induced vibrations; long-span bridges; aerodynamic models; buffeting analysis.

## 1. Introduction

The life cycle of a life-line structure such as along-span bridge is an integrative process in which each stage of its existence has to be checked thoroughly, starting from its construction, up to the designed life-period. In the construction stage, the structural system of a bridge differs from in-service design, leading to additional design checks performed in critical erection conditions. In case of long-span flexible bridges these checks are commonly conducted against critical wind-induced vibrations. This ensures safety and serviceability throughout construction and in-service by limiting the response from which residual forces are stored into the structure. The Fluid-Structure Interaction (FSI) due to gusty wind is a complex phenomenon, which is described by several approaches and models. In case of bridge decks, the FSI is simulated by wind-tunnel experiments, semi-analytical models based on the theory of aero elasticity supplemented by wind tunnel deliverables and the numerical approaches using Computational Fluid Dynamics (CFD) have gotten considerable attention within the last two decades. With different sets of assumptions, the semi-analytical models are based on the analytical solution from flat-plate aerodynamics. By an introduction of modification coefficients based on experiments, they model the complex unsteady behavior of bluff bodies. The two main theories under which these models are developed are the quasi-steady theory and the linearized unsteady theory. The quasi-steady theory neglects the fluid memory and unsteadiness of the wind and it takes into account the aerodynamic nonlinearities by utilizing the nonlinear static wind coefficients. The linearized unsteady theory separates the aerodynamic forces into static, self-excited and buffeting force components in order to unveil the complex behaviour of bluff body aerodynamics. With this, the unsteadiness of the buffeting and the self-excited forces is considered to be dependent on the frequency of the wind-signal and structural motion, respectively. The models are taking into account the fluid memory corresponding to the delay of the buffeting and self-excited forces due to periodic gust action and motion of the bluff body through frequency dependent coefficients. In case of self-excited forces, these are commonly addressed as flutter derivatives [1] and for the buffeting forces as aerodynamic admittance functions. These coefficients are derived analytically for flat plate based on potential flow. Another point which is of imperative importance in aerodynamic modelling is the aerodynamic coupling between

modes, which is the main cause of flutter instability. For high wind speeds, energy transfer between modes occurs due to the motion of the structure, which after a certain threshold results in divergent amplitudes of oscillations. Within the scope of this work, the main aspect is to evaluate the assumptions which implied in different semi-analytical models for a cable-stayed bridge in the erection stage with free cantilever of 205m and to quantify their importance: which model should be sufficient to analyse this type of structure for design wind speeds. Additionally, it represents a simplified model for lower wind-speeds, neglecting the aerodynamic coupling between modes and wind fluctuations for structures with low frequencies where resonant part is dominant over the background turbulence.

## 2. Aerodynamic models

The wind-structure interaction is a complex 3D phenomenon, originating from the nature of the turbulence. However, most of the aerodynamic models are developed for 2D sectional models, which are then applied to a 3D structure in order to simulate the full behaviour. Some studies [2] consider the span-wise correlation between the wind forces introducing empirical join-acceptance functions; however, this will not be considered in this case. The governing equations of motions of a 3D linear structure in matrix notation using the computationally efficient mode generalized approach are given by:

$$M\ddot{\boldsymbol{q}} + C\dot{\boldsymbol{q}} + K\boldsymbol{q} = \boldsymbol{f}. \tag{1}$$

Here, $M = \Psi^T M_0 \Psi$, $C = \Psi^T C_0 \Psi$ and $K = \Psi^T K_0 \Psi$ are the modal mass, damping, and stiffness matrices respectively, obtained from the full system matrices $M_0$, $C_0$ and $K_0$ and the mode shape matrix $\Psi$; $\boldsymbol{q} = \Psi^T \boldsymbol{x}$ are the generalized displacements with its time derivatives $\ddot{\boldsymbol{q}}, \dot{\boldsymbol{q}}$. The generalized force $\boldsymbol{f} = \Psi^T \boldsymbol{f_0}$ represents the aerodynamic loading, including the static, buffeting and self-excited component, which in case of non-linear aerodynamic loading cannot be separated. On Figure 1 a simplified 3 Degree-of-Freedom (DOF) bridge deck is presented for which the system force vector $\boldsymbol{f_0} = [F_D F_L F_M]^T$ includes the drag, lift and moment component respectively and the displacement vector is constituted of horizontal and vertical displacement and rotation $\boldsymbol{x} = [ph\alpha]^T$. The width of the bridge deck is denoted as $B$ and the wind is acting with mean wind speed $U$, and fluctuating components $u$ and $w$ in horizontal and vertical direction respectively.

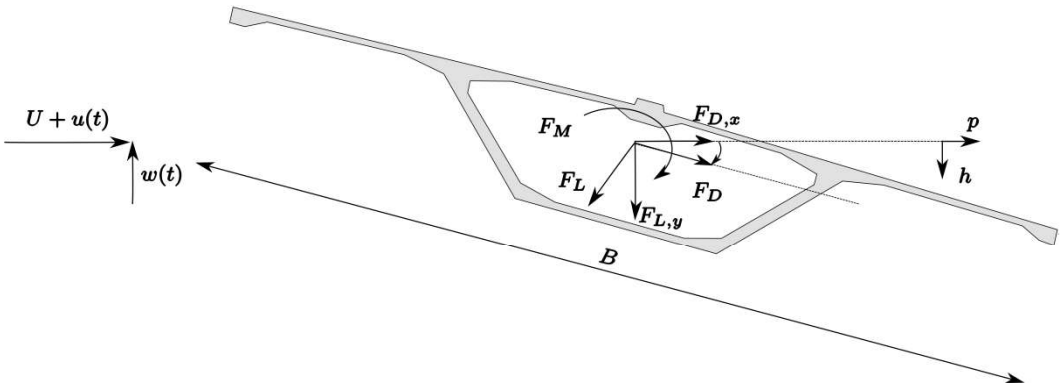


*Figure 1: Aerodynamic forces on bridge deck section including sign conventions.*

### 2.1 Quasi-Steady (QS), Linearized Quasi-Steady (LQS) and Corrected Quasi-Steady(CQS) model

The quasi-steady theory is based on the assumption that in each time-step the fluid-structure interaction is the same as in an equivalent steady state of a certain point of the bridge deck. With this, the rise-time of the aerodynamic forces is assumed to be instantaneous and the fluid memory effect is not considered. Additionally, it assumes full correlation of the forces; thus, the aerodynamic admittance is unitary. The main advantage of this theory is the consideration of the aerodynamic nonlinearity: the value of the wind coefficients depends on the instantaneous angle of

attack considering wind fluctuations and structural motion. The net forces acting on a bridge deck are:

$$F_D = \frac{1}{2}\rho V_{rel,D}^2 B C_D(\alpha_{r,h}), F_L = -\frac{1}{2}\rho V_{rel,L}^2 B C_L(\alpha_{r,h}), \quad F_M = \frac{1}{2}\rho V_{rel,M}^2 B^2 C_M(\alpha_{r,\theta}), \qquad (2(a,b,c))$$

where $C_D, C_L$ and $C_M$ are the static drag, lift and moment coefficients respectively. The relative wind velocity$V_{rel,i}$ is computed taking into account the bridge displacements as

$$V_{rel,i} = \sqrt{(U + u - \dot{p})^2 + (w + \dot{h} + m_{r,i} B\dot{\alpha})^2}. \qquad (3)$$

The total angle of attack in this case is calculated from the static angle of equilibrium $\alpha_0$, the instantaneous rotation of the bridge deck $\alpha$ and the dynamic angle of attack $\varphi$

$$\alpha_{r,i} = \alpha_0 + \alpha + \varphi = \alpha_0 + \alpha + \frac{(w + \dot{h} + m_{r,i} B\dot{\alpha})}{U + u - \dot{p}}. \qquad (4)$$

The quasi-steady lift force is computed at the cross section with integration of the circulation around the body. The factor $m_{r,i}$ for$i \in (D, L, M)$represents the position of the aerodynamic centre where the lift force is applied due to torsional motion. In this study it was taken as 0.25 for the vertical DOF and as -0.25 for the torsion, as it introduces positive aerodynamic damping for low reduced velocities in case 0.25 is used for torsion, which is the case for a flat plate.

Diana in [3] introduced the dynamic derivatives by correction coefficient $k_i$ in order to take into account the unsteady effects. With this the static wind coefficients in eq. 2 are replaced by dynamic ones $K_i$, for different angles of incidence as

$$K_i = C_i(\alpha_0) + \int_{\alpha_0}^{\alpha_{r,i}} k_i \, C_i^{'} \, d\alpha, \qquad (5)$$

where$C_i^{'}$ is the derivative of the static wind coefficient$i$at a certain angle. The correction coefficient $k_i$ is determined ether from wind tunnel testing, or the flutter derivatives for a certain frequency equating the linearized QS to the semi-empirical model, as computed in this case.

The forces computed with the quasi-steady theory are then transformed with respect to the bridge coordinate system, using standard coordinate transformation with respect to the dynamic angle of attack. Commonly the static wind coefficients from wind-tunnel experiments are given up to certain angle of attack (±5deg.) including the slope of the static wind coefficients. In that case, a linearized model with respect to the static angle of attack is developed, simply by employing Taylor's approximation on equation (3) and the hypothesis of small angles of attack i.e. neglecting the multiplication of the fluctuation terms. The linearized quasi-steady model is then obtained as:

$$F_{D,x} = \frac{1}{2}\rho U^2 B \left( C_D + (C_D^{'} - C_L)\frac{w}{U} + C_D \frac{2u}{U} + (C_D^{'} - C_L)\frac{\dot{h} + m_{r,h} B\dot{\alpha}}{U} + C_D^{'}\alpha - 2C_D \frac{\dot{p}}{U} \right), \qquad (6a)$$

$$F_{L,y} = -\frac{1}{2}\rho U^2 B \left( C_L + (C_L^{'} + C_D)\frac{w}{U} + C_L \frac{2u}{U} + (C_L^{'} + C_D)\frac{\dot{h} + m_{r,h} B\dot{\alpha}}{U} + C_L^{'}\alpha - 2C_L \frac{\dot{p}}{U} \right), \qquad (6b)$$

$$F_M = \frac{1}{2}\rho U^2 B^2 \left( C_M + C_M^{'}\frac{w}{U} + C_M \frac{2u}{U} + C_M^{'}\frac{\dot{h} + m_{r,h} B\dot{\alpha}}{U} + C_M^{'}\alpha - 2C_M \frac{\dot{p}}{U} \right). \qquad (6c)$$

## 2.2 Linearized Semi-Analytical(LSA) modeland Modified Quasi-Steady (MQS) model

The models based on the quasi-steady theory do not take into account the unsteady behaviour of the bluff body under laminar or turbulent wind. CQS does up to some extend by the coefficient $K_i$; however, this coefficient does not cover the whole frequency range. The situation in reality is rather more complex and the motion has a broad band of frequencies, therefore Scanlan [1] developed a model for the self-excited forces including frequency dependent coefficients, i.e. the flutter derivatives. With these, the aerodynamic forces are described as linear function of the motion and its frequency content including the aerodynamic coupling among modes of vibrations. This is of particular interest at high wind velocities, where flutter occurs. The LSA model is developed based on linearized forces at the static angle of attack and represents a superposition of buffeting, static and self-excited forces. The self-excited forces per unit span in the extended Scanlan's format are represented as:

$$F_{D,x}^{se} = \frac{1}{2}\rho U^2 B\left(KP_1^*\frac{\dot{h}}{U} + KP_2^*\frac{\dot{\alpha}}{U} + K^2P_3^*\alpha + K^2P_4^*\frac{\dot{h}}{U} + KH_5^*\frac{\dot{p}}{U} + K^2H_6^*\frac{p}{B}\right), \quad (7a)$$

$$F_{L,y}^{se} = \frac{1}{2}\rho U^2 B\left(KH_1^*\frac{\dot{h}}{U} + KH_2^*\frac{\dot{\alpha}}{U} + K^2H_3^*\alpha + K^2H_4^*\frac{\dot{h}}{U} + KH_5^*\frac{\dot{p}}{U} + K^2H_6^*\frac{p}{B}\right), \quad (7b)$$

$$F_M^{se} = \frac{1}{2}\rho U^2 B^2\left(KA_1^*\frac{\dot{h}}{U} + KA_2^*\frac{\dot{\alpha}}{U} + K^2A_3^*\alpha + K^2A_4^*\frac{\dot{h}}{U} + KA_5^*\frac{\dot{p}}{U} + K^2A_6^*\frac{p}{B}\right), \quad (7c)$$

where $P_i^*(K), H_i^*(K)$ and $A_i^*(K)$ for $i \in (1,2,3,4)$ are the flutter derivatives dependent on the reduced frequency $K = {\omega B}/{U}$, $\omega$ being circular frequency of oscillation.The buffeting forces, including the static wind component, are introduced as:

$$F_{D,x}^{b} = \frac{1}{2}\rho U^2 B\left(C_D + (C_D^{'} - C_L)\frac{w}{U}\chi_{L,w} + C_L\frac{2u}{U}\chi_{L,u}\right), \quad (8a)$$

$$F_{L,y}^{b} = -\frac{1}{2}\rho U^2 B\left(C_L + (C_L^{'} + C_D)\frac{w}{U}\chi_{D,w} + C_D\frac{2u}{U}\chi_{D,u}\right), \quad (8b)$$

$$F_M^{b} = \frac{1}{2}\rho U^2 B^2\left(C_M + C_M^{'}\frac{w}{U}\chi_{M,w} + C_M\frac{2u}{U}\chi_{M,u}\right). \quad (8c)$$

To cover the unsteady effects the aerodynamic admittance functions $\chi_{i,j}(K)$ are introduced to cover the unsteady effects and the deck-wise correlation. This model neglects the aerodynamic nonlinear effect; however, it takes the fluid memory into account. These relations are of mixed nature i.e. they contain frequency and time-dependent terms and in order to be able to solve them in time domain, rational function approximation is required. In this case the impulse functions based rational approximation was utilized.

The Modified Quasi-Steady (MQS) model developed in [4], approximates the aerodynamic derivatives at the natural modal frequencies resulting in frequency independent self-excited forces. In this work, additionally the buffeting forces are approximated in the same manner, by utilizing each frequency in order to obtain frequency independent terms. Considering response of single mode $m$, for well separated modes the PSD of the displacements due to wind fluctuation

$$S_{z,mm}(\bar{\omega}) = \varphi_m^2 |H_{mm}(i\bar{\omega})|^2\left(\left|H_{w,mm}(i\bar{\omega})\right|^2 S_w(\bar{\omega}) + \left|H_{u,mm}(i\bar{\omega})\right|^2 S_u(\bar{\omega})\right), \quad (11)$$

where $S_{z,mm}(\bar{\omega})$ is the PSD of the vertical displacement of the $m$ mode including the mechanical admittance function including decoupled aerodynamic terms $H_{mm}(i\bar{\omega})$ . $H_{w,mm}(i\bar{\omega})$ and $H_{u,mm}(i\bar{\omega})$represent the transfer functions between vertical and horizontal fluctuations and buffeting force including the aerodynamic admittance, pressure and static wind coefficients. In this case the aerodynamic coupling between the self-excited forces is neglected, as well as the cross spectral density of the generalized buffeting forces. Although the admittance functions are transfer functions between the wind fluctuations and buffeting forces and are indeed completely independent of the frequency of the system, the main interest are the displacements. If further assumed that the resonant part is dominant over the background part of the turbulence, which is justified only for structures with low dominant structural frequencies, the mechanical admittance is narrowband. With this assumption, the aerodynamic admittance and flutter derivatives become functions of only one frequency i.e. $P_i^*(K) = P_{i,m}^*(K_m), H_i^*(K)$and $A_i^*(K) = A_i^*(K_m)$from eq. (7)and $\chi_{i,j}(K) = \chi_{i,j,m}(K_m)$from eq. (8).As the reduced velocity increases, the aerodynamic damping increases as well, leading to a significant contribution of the non-stationary terms of the damping forces. This corresponds to wider brand of PSD of the response resulting in increment of the error considering a single frequency. The advantage of this model is that the implementation is rather simple with low computational costs.

### 2.3 **Hybrid Nonlinear (HNL) model**

The motivation of the hybrid model developed by Chen [2] is to utilize the advantages offered by the different aerodynamic models for different reduced velocities. The response and the wind-spectrum are separated by demarcation on the frequency content on low and high frequency component. The lower frequency component of the wind is solved using the QS model resulting in

low frequency effective angle of incidence, at which the high frequency component is linearized using the LSE model. The total forcing on the system is then computed as

$$F = F_{QS}(\alpha_r^l) + F_{LSA}\big|_{\alpha_r^l}, \tag{12}$$

where$F_{QS}(\alpha_r^l)$is the quasi steady forcing from lower frequency wind component (eq.2)and $F_{LSA}$ is the linearized semi-analytical (eqs. 7 and 8) at effective angle of incidence from lower frequency fluctuation and motion. With this, the aerodynamic nonlinearities are covered by the QS model and since the unsteady characteristics are distinctive for the high reduced velocity, the LSE model is used to capture the fluid-memory effect. The wind-velocity fluctuations are separated using digital filter on low and high frequency components. In this model, flutter derivatives for different angles are necessary.

# 3. Application

In the design procedure of long-span bridges, the erection stage is of particular interest as the structural system substantially differs from the final form of the structure. Suitable design criteria need to be established as basis during construction, which are commonly lower than in-service stagedue to the lower exposure period. The reference object for this study is a segment of a multi-span cable-stayed bridge depicted in Figure 2, erected by the traditional balanced cantilevering method. The models described above are applied in order to obtain the structural response due to wind action, which commonly represents the major criterion for design.

## 3.1 Structural system

The two cantilevers on each side of the tower are 205m long with 33.15 m wide and 4.85m deep concrete box section (Figure 1), as depicted in Figure 2with additional properties listed in Table 1,including mass per meter length of the deck including cables. The inherent property of this type of girders is their high sectional modulus which results in rather high structural stiffness compared to light streamlined sections. Taking this into account, modal properties of the first three deck natural frequencies are rather higher compared to flexible cable stayed bridges. It should be noted that additional tower modes were also included in the analysis with a total of fifteen modes of vibration.

*Table 1: Basic structural data and modal properties.*

| Mass [t/m] | Inertial mass [$tm^2/m$] | Lateral freq. [Hz] | Vertical freq. [Hz] | Torsional freq. [Hz] | Damping ratio [-] |
|---|---|---|---|---|---|
| 28.71 | 2991.99 | 0.401 | 0.444 | 0.913 | 0.01 |

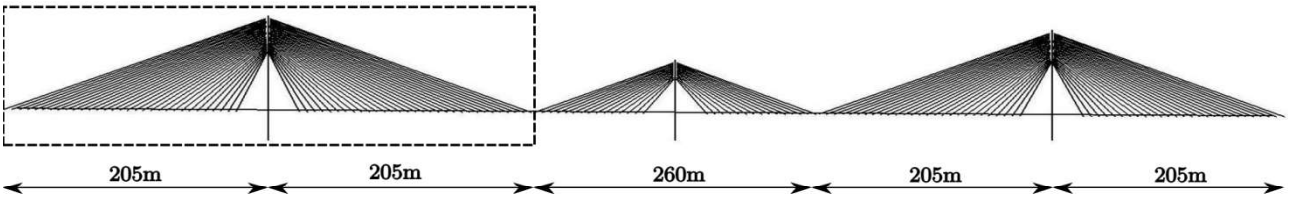


*Figure 2: Reference object: West tower in erection stage.*

## 3.2 Aerodynamic section properties

The static wind coefficients, depicted in Figure 3, and the flutter derivatives were obtained utilizing the computationally efficient CFD code, VX flow, based on the Vortex Particle Method, developed and validated by Morgenthal [5].The flutter derivatives are obtained for different angle of incidence and are depicted in Figure 4. Bluff box girders are usually prone to torsional flutter, and their flutter derivatives are rather irregular and sensitive on the angle of incidence. For irregular patterns of the flutter derivatives with respect to thin airfoil, rational approximation can be cumbersome.

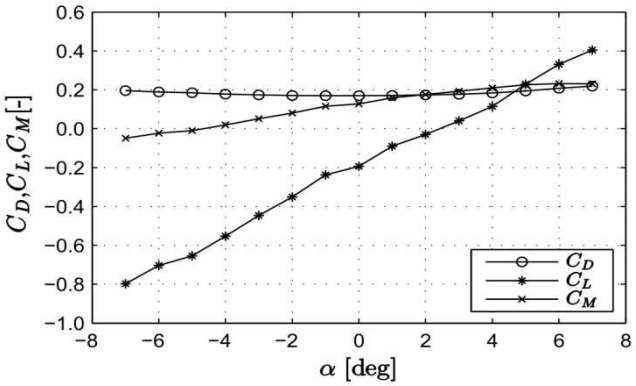


*Figure 3: Static wind coefficients.*

With the introduction of additional aerodynamic states, the rational function was conveyed resulting in rational functions, as depicted in Figure 4. Particular difficulty was encountered in obtaining the exact point of changing signs of $A_2^*$ for 6 deg. in order to be able to predict reliably the torsional flutter limit. Therefore, for only in this case, four aerodynamic coefficients were introduced in the rational approximation. The flutter limit is looked at in the following sections. Although with the introduction of additional states in the rational approximation a better fit of the curved is obtained, the extrapolation for high reduced velocities leads to deviation from steady-state forces. Thus the key point is the balance in selecting aerodynamic states for simulation of the rise time of the aerodynamic forces and their final quasi-steady form. Sears's function was used for the six aerodynamic admittance functions, i.e. it was considered as uniform.

### 3.3 **Aerodynamic analysis**

The structure was subjected to a 600s period of wind, generated with a 0.01 s time step, for seven different wind-speeds ranging from 25 m/s to 75 m/s for two different levels of turbulence intensity – a lower one $[I_u I_w]$=[15% 12%] and a higher one $[I_u I_w]$ = [25% 20%]. The Root-Mean-Square (RMS) from the vertical displacement and rotation for wind speed of 75 m/s are depicted in Figure 5.

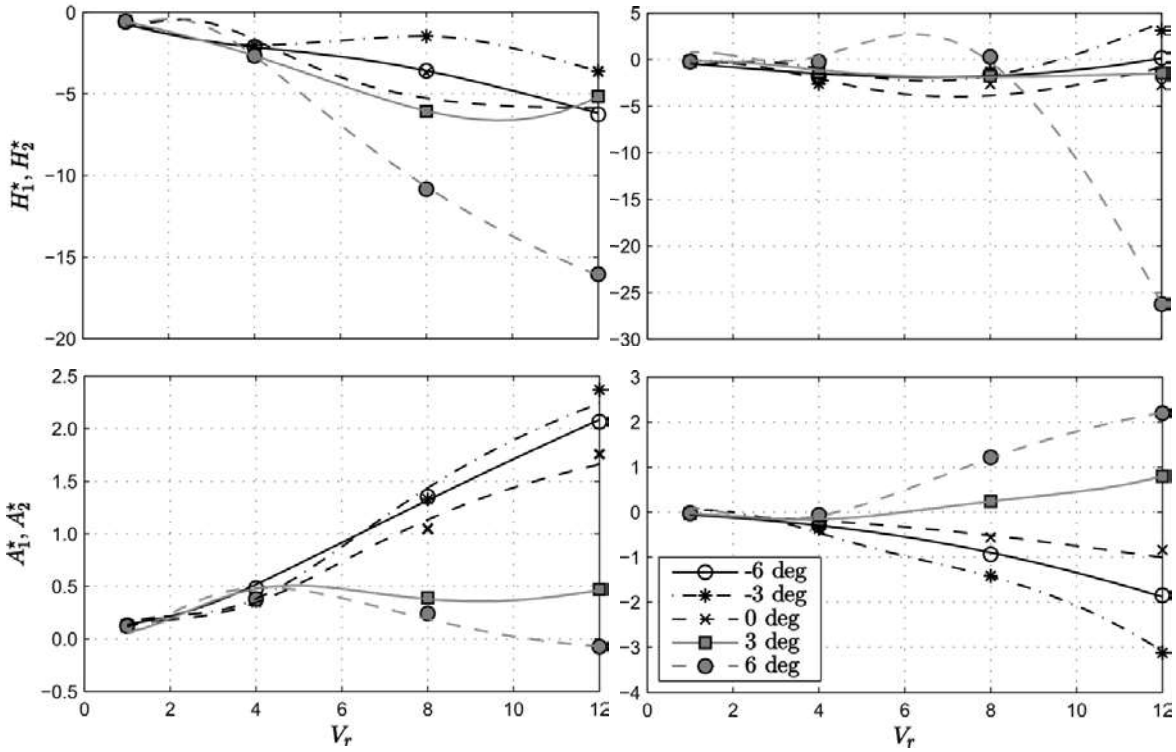


*Figure 4: Aerodynamic derivatives for different angle of incidence: Values at markers are from CFD; the lines represent the rational approximation.*

Three main branches could be distinguished: first one with highest amplitudes without any self-excited forces, introduced by the Steady Theory (ST) and Linearized Steady Theory (LST) models. The second one contains all of the previously described models without the consideration of the aerodynamic admittance and the last one, including Sears admittance denoted by subscript "s". The difference is substantial for the models including self-excited forces with admittance and without the consideration of them, as seen for the second and third branch. The branches tend to diverge with the increment of the turbulence intensity, as the self-excited forces rise with the magnitude of the response as well. Comparing the effect of aerodynamic admittance, considerable differences are noted. In realistic situation, the aerodynamic admittance differs from the theoretical one for flat plate; however, it could as also include overshooting effect in the rise-time of the gust induced force which actually would result in rise in the response of the structure. Looking at the models in the second branch, on Figure 5, the QS and CQS seem to give the highest amplitude. Although CQS should take fluid memory into account, which would effectively decrease the response, a considerable amount of ambiguity is implied in obtaining this factor from the flutter derivatives, especially if it is considerably greater than 1. This would effectively increase the slope of the lift coefficient, leading to high amplitudes. From the good agreement between MQS and LSA, a conclusion could be driven that the aerodynamic coupling for this case and under these specific wind-speeds is insignificant. Utilizing the MQS, a considerably less computational effort is required and a numerical uncertainty in rational approximation is avoided. Usually the aerodynamic nonlinearity decreases the response since the slope of the lift is lower for higher angles. However, in this case the QS resulted in higher vertical response, since the contribution of the projected drag force was higher compared to the LQS where only the derivative of the drag coefficient was used.

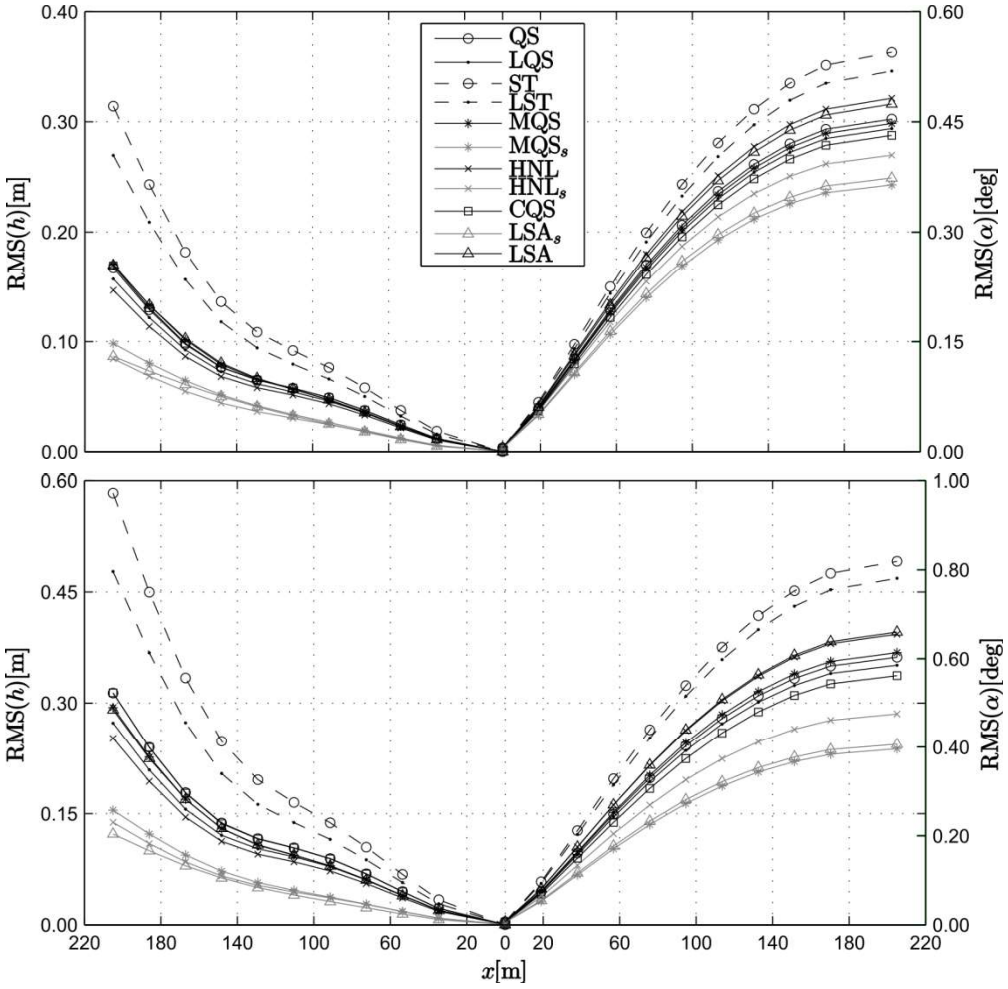


*Figure 5: RMS of vertical displacement (left) and rotation (right) at U=75m/s. Top is for turbulence* $[I_u I_w]$ *= [15% 12%] and bottom* $[I_u I_w]$ *= [25% 20%]. Acronyms are explained through the text.*

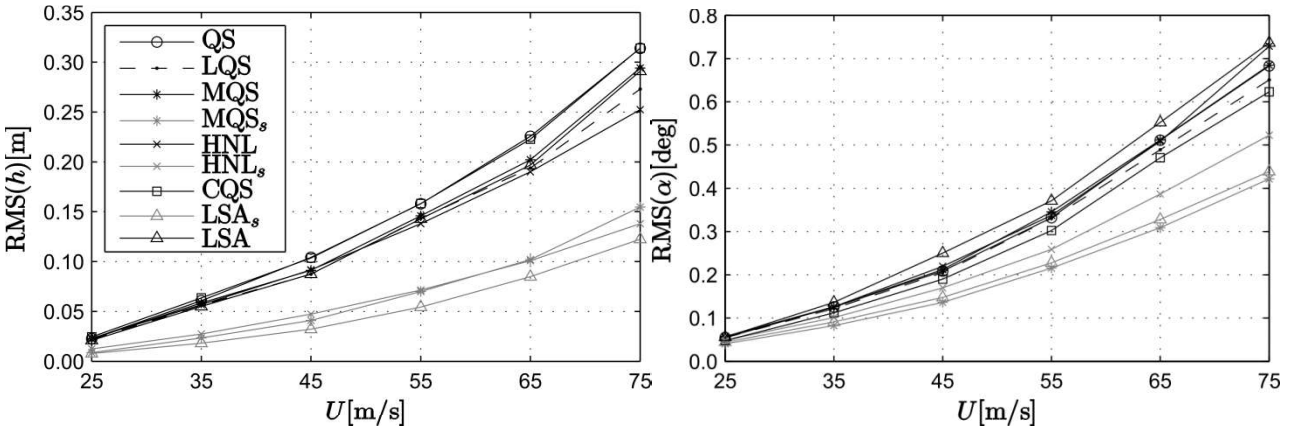


*Figure 6: RMS of vertical displacement (left) and rotation (right) of cantilever tip.*

The introduced model $MQS_s$ with decoupled admittance seems to have good trend for the rotational degree of freedom. In case of vertical displacement, the larger contribution of background turbulence results in higher discrepancy with $LSA_s$. A particular point of interest represents the behaviour of the NHL model, which decreases the response for the vertical displacements, and increases in case of rotations. This is owed to the significant reduction in the aerodynamic damping in the torsional motion in the $A_2^*$ derivative depicted on Figure 4. The flutter limit for box girders with side cantilevers is sensitive to the angle of incidence. With the change of the sign of the same coefficient for 6 deg., positive aerodynamic damping is induced causing torsional flutter for $V_r \geq 4.5$ (Table 2). Although torsional flutter dominates the motion, there is a slight difference to the flutter limit due to aerodynamic coupling, which explains the difference between the MQS with its analytical solution (flutter for torsional DOF) and LSA. For 0 deg., flutter does not occur up to 180 m/s. Higher wind speeds were not considered since extrapolation is necessary of flutter derivatives.

*Table 2: Flutter limit$U_{cr}$ [m/s] with different approaches for 6 deg. angle.*

| Analytical MQS | MQS | LSA | LSA (freq. domain) |
|---|---|---|---|
| 134.2 | 134.2 | 128.0 | 128.8 |

# 4. Conclusion

Various models for buffeting analysis were presented and their implied assumptions were quantified for a particular bridge in the erection stage. The influence of the self-excited forces and the aerodynamic admittance was proven to be more significant in the design velocity ranges in this followed by the fluid memory, aerodynamic nonlinearity and with minor effect of aerodynamic coupling. With the increment of the complexity of the model, models are able to reproduce more phenomena occurring in the FSI; however, numerical and parameter uncertainties arise. For preliminary checks in the erection condition, where smaller wind loads are applied, less complex models such as MQS and even QS could be employed for initial assessment. However, the final check of the design more complex models should be utilized, such as LSA and HNL. This could be also avoided if LSA is solved in frequency domain. In conclusion, the model choice is highly dependent on the case study, and it is in the designers' interest to evaluate various models based on their assumptions and the available aerodynamic properties, in order to obtain reliable estimate.

## References

[1] SIMIU E., and SCANLAN R., *Wind Effects on Structures*. Wiley New York, 1996.
*[2] CHEN X., and KAREEM, A.,* "Aeroelastic analysis of bridges: Effects of turbulence and aerodynamic nonlinearities", *Journal of Engineering Mechanics,* Vol 129, 2003, pp. 885-895.
[3]DIANA G., BRUNI S., CIGADA A., and COLLINA A., "Turbulence effect on flutter velocity in long span suspended bridges", *Journal of Wind Engineering and Industrial Aerodynamics,* Vol. *48, 1993, pp.329-341.*
[4] ØISETH O., RÖNNQUIST A., and SIGBJÖRNSSON R., "Time domain modeling of self-excited aerodynamic forces for cable-supported bridges: A comparative study", *Journal of Computer and Structures,* Vol 89, 2011, pp 1306-1322.
[5] MORGENTHAL G., *Aerodynamic Analysis of Structures using High-resolution Vortex Particle Methods*, PhD Thesis, University of Cambridge, 2002.
[6] WU T., and KAREEM, A., "Bridge aerodynamics and aeroelasticity: A comparison of modeling schemes", *Journal of Fluids and Structures,* Vol 43, 2013 pp.347-370.